*Carbohydrate Research*, 245 (1993) 113–128
Elsevier Science Publishers B.V., Amsterdam



# NMR studies of oligosaccharides derived from hyaluronate: complete assignment of $^{1}H$ and $^{13}C$ NMR spectra of aqueous di- and tetra-saccharides, and comparison of chemical shifts for oligosaccharides of increasing degree of polymerisation

Renato Toffanin [a], Bjarne J. Kvam [a,*], Antonella Flaibani [a], Marco Atzori [a], Filippo Biviano [b], and Sergio Paoletti [a,c]

[a] *Centro Ricerche POLY-biòs, LBT – Area di Ricerca, Padriciano 99, I-34012 Trieste (Italy)*
[b] *FIDIA Research Laboratories, FIDIA S.p.A., Via Ponte della Fabbrica 3/A, I-35031 Abano Terme (Italy)*
[c] *Dipartimento di Biochimica, Biofisica e Chimica delle Macromolecole, Università degli Studi di Trieste, Via L. Giorgieri 1, I-34127 Trieste (Italy)*

(Received October 29th, 1992; accepted January 6th, 1993)

## ABSTRACT

A series of oligosaccharides was prepared from hyaluronate by depolymerisation with bovine testicular hyaluronidase. Complete assignment of the $^{1}H$ and $^{13}C$ NMR spectra was obtained for the disaccharide, the tetrasaccharide, and the $NaBH_4$-treated tetrasaccharide, by using various 1D and 2D NMR methods. The $^{1}H$ assignments for the tetrasaccharide differ from the incomplete data reported recently (ref. 11). The $^{13}C$ NMR spectra of the aqueous di-, tetra-, hexa-, and octa-saccharides of this series show that all resonances, apart from those subject to obvious end effects, have chemical shifts comparable to those of the corresponding resonances of hyaluronate in $D_2O$. The observed $^{13}C$ chemical shifts suggests that cooperative intramolecular hydrogen bonds probably play a minor role in determining the conformation of hyaluronate in water.

## INTRODUCTION

Hyaluronate {→4)-β-D-Glc*p*A-(1→3)-β-D-Glc*p*NAc-(1→}$_n$ is biologically important as a structural material in cartilage[1] and vitreous humour[2], and serves as a lubricant[3] and free-radical scavenger[4] in synovial fluid. Apart from these rather mechanical roles, it has been shown that certain low molecular weight hyaluronate fractions stimulate angiogenesis[5]. A series of oligosaccharides derived from hyaluronate has been studied in solution in methyl sulfoxide[6–9], leading to assignment of the majority of the resonances, although overlapping signals prevented

* Corresponding author.

complete assignment by 1D NMR methods. Studies of the NH resonances of oligomers of various lengths in $H_2O$ have been undertaken in order to shed light on the hydrogen bond pattern[10]. In recent work dealing with various types of hyaluronidases and their products, a partial assignment of the $^1H$ NMR spectrum of the tetrasaccharide β-D-Glc*p*A-(1 → 3)-β-D-Glc*p*NAc-(1 → 4)-β-D-Glc*p*A-(1 → 3)-D-Glc*p*NAc in $D_2O$ was presented[11]. However, these authors provided neither *J* values nor $^{13}C$ NMR chemical shifts, and several of their assignments are at variance with our present findings.

It can be inferred from published results that the conformations of hyaluronate in aqueous solution[9,10] and in methyl sulfoxide[8,12] differ more than previously thought[8]. In order to examine this hypothesis further, and in the light of the reported biochemical effect of short hyaluronate fragments[5], we have undertaken NMR studies of a series of even-numbered oligosaccharides derived from hyaluronate. The work was aimed at the complete assignment of the $^1H$ and $^{13}C$ NMR spectra for the disaccharide β-D-Glc*p*A-(1 → 3)-D-Glc*p*NAc (**1**), the tetrasaccharide β-D-Glc*p*A-(1 → 3)-β-D-Glc*p*NAc-(1 → 4)-β-D-Glc*p*A-(1 → 3)-D-Glc*p*NAc (**2**), and its corresponding reduced form obtained by $NaBH_4$ reduction, β-D-Glc*p*A-(1 → 3)-β-D-Glc*p*NAc-(1 → 4)-β-D-Glc*p*A-(1 → 3)-2-acetamido-2-deoxy-D-glucitol (**3**). Based on these assignments, spectra of oligosaccharides of different chain length were compared and examined for signs of conformational cooperativity.

## EXPERIMENTAL

*Methods.*—$^1H$ NMR and $^{13}C$ NMR experiments were performed at 4.70, 7.05, and 11.74 T on Bruker AC 200, AM 300 WB, AMX and AM 500 instruments ($^1H$: 200, 300, and 500 MHz; $^{13}C$: 50.3, 75.4, and 125.7 MHz), respectively. The sample temperature was 25°C and the sample concentration was 30 mg/mL, unless stated otherwise. Chemical shifts are with reference to internal acetone ($^1H$, 2.225 ppm; $^{13}C$, 31.07 ppm). Typically, COSY45 data were acquired using 32 scans per series in 1 and 0.5 k data points in $F_2$ and $F_1$, respectively, with zero-filling in $F_1$. Centred sine-bell weighting was applied prior to Fourier transformation. $^1H$–$^{13}C$ chemical shift correlation data were acquired with $^1H$-detection via heteronuclear multiple-quantum coherence (HMQC)[13] on a Bruker AMX 500 instrument. A matrix of 256 × 1024 data points was applied, using squared sine-bell weighting functions prior to Fourier transformation. All pulse sequences for 2D experiments were standard Bruker software.

*Simulation of spectra.*—Simulation and fitting of the 500-MHz $^1H$ NMR spectra was performed with the PANIC simulation software (a modified version of the LAOCN3 programme[14]) running on the ASPECT 3000 computer of the NMR spectrometer.

*Materials.*—Enzymatic digestion of hyaluronate by testicular hyaluronidase results in cleavage of the (1 → 4)-glycosidic bond[15]. The principal end-products are the tetra- and hexa-saccharides, but also a small proportion of disaccharide is

formed[15]. For the preparation of the tetrasaccharide **2**, purified rooster-comb sodium hyaluronate (500 mg, FIDIA, Abano Terme, Italy) was dissolved in aq NaCl (0.15 M, 50 mL), buffered with NaOAc–HOAc (0.1 M, pH 5.0). After preincubation of the hyaluronate solution at 37°C for 0.5 h, 1 mL of bovine testicular hyaluronidase (EC 3.2.1.35, Sigma, 980 U/mg) dissolved in the same buffer (50 mg in 4 mL) was added, with further aliquots of 1 mL added after 1 and 5 h. The digestion was terminated after 48 h by heating to 100°C for 5 min. After cooling, the protein was removed by centrifugation for 20 min. The supernatant solution was concentrated to dryness, redissolved in 10 mL of distilled water, and subjected to chromatography on a DEAE-Sephacel (Pharmacia) ion-exchange column (2.5 × 60 cm), equilibrated with 0.01 M $Na_2SO_4$. The eluent flow was 25 mL/h, and a linear $Na_2SO_4$ gradient (0.01–0.2 M/24 h) was applied. The chromatography was monitored with a UV detector (Jasco UVDEC 100 V) at 216 nm. The fractions were screened for uronic acids using the *m*-hydroxybiphenyl assay[16]. Appropriate fractions were pooled, concentrated, desalted on a Bio-Gel P-2 column (1.5 × 40 cm, Bio-Rad Laboratories), and lyophilised. The procedure described yielded mainly tetra- and hexa-saccharides in significant amounts. The octasaccharide was produced by using less enzyme.

The disaccharide **1** was prepared essentially as described for the longer oligosaccharides, using a higher polysaccharide-to-enzyme ratio (20:1, w:w). The hyaluronate was added to the enzyme solution (5 mg/mL), to a final concentration of 100 mg/mL. After 24-h digestion, the enzyme was deactivated and removed by filtration. The pH was adjusted to 7, and the digest was subjected to ion-exchange chromatography on a DEAE-Sephadex CL-6B column (3 × 60 cm) at 4°C. Elution was performed first with phosphate buffer (0.01 M, pH 7, 1.2 L) containing EtOH (2%), then with 0.03 M NaCl containing EtOH (2%). The fractions were analysed for uronic acids by the carbazole method[17]. Appropriate fractions were pooled, and converted into the tetrabutylammonium salt form (Bio-Rad AG50W-X8, $TBA^+$-form). The disaccharide was desalted by dialysis (Amicon membrane dialyser; cut-off, 500), converted into the Na-form (Bio-Rad AG50W-X8, $Na^+$-form), and then recovered by lyophilisation.

The reduced tetrasaccharide **3** was prepared as follows: tetrasaccharide **2** (100 mg) was dissolved in distilled water (10 mL), and 2.5 mL of aq $NaBH_4$ (1%, w/w) was added. After reaction at room temperature overnight, the excess of hydride was decomposed by adding concd HOAc. The mixture was concentrated to dryness, washed and concentrated repeatedly with 10% HOAc in MeOH and finally with MeOH, to remove residual borate. The reduced tetrasaccharide **3** was re-dissolved in water, converted into the acid form by ion exchange on Amberlite IR-120 resin ($H^+$-form), and lyophilised.

## RESULTS

*Assignment of NMR spectra.*—In Figs. 1 and 2, the 300-MHz COSY plots obtained for $D_2O$ solutions of the disaccharide **1** and the tetrasaccharide **2**,

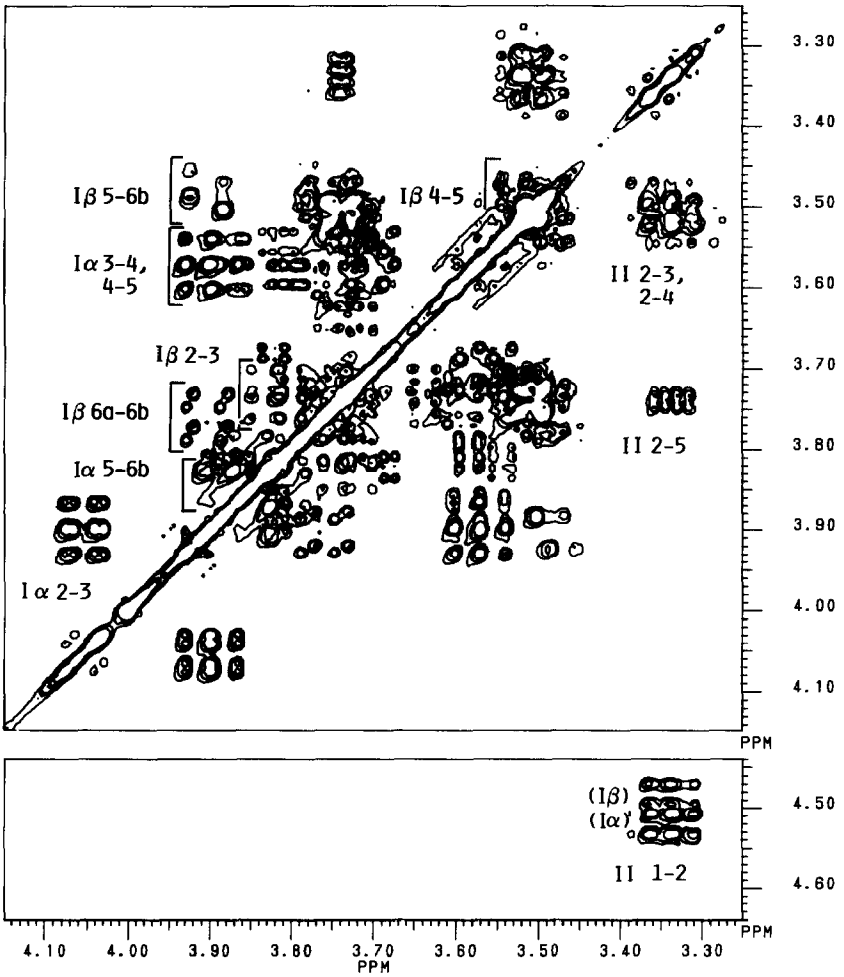


Fig. 1. 300-MHz $^1H$–$^1H$ COSY45 plot obtained at 25°C for a $D_2O$ solution of the disaccharide **1** (10 mg/mL). Residues are numbered from the reducing end with Roman numerals, i.e., I (above diagonal) and II (below diagonal) denote Glc*p*NAc and Glc*p*A correlations, respectively. The Glc*p*NAc H-1 and Ac signals are omitted.

respectively, are shown. The testicular hyaluronidase gives oligosaccharides with GlcNAc residues at the reducing end[15]. This is evident from the presence of the $\alpha$- and $\beta$-form resonances for the Glc*p*NAc I residues, as seen in the COSY plots (see Figs. 1 and 2, residues are numbered from the reducing end with Roman numerals). The anomeric equilibrium is reflected also in the H-1 resonance of the adjacent Glc*p*A II residues. All resonances for **1**, apart from those of I$\beta$ H-4 and I$\alpha$ H-6a,6b, could be identified from the COSY plot (Fig. 1). These assignments facilitated the identification of the cross-peaks for **2**. Useful for comparison were also the COSY plots for **3** in neutral and acid form. The absence of the reducing-end signals allowed, e.g., the Glc*p*NAc III signals of **3** to be identified. In the acid

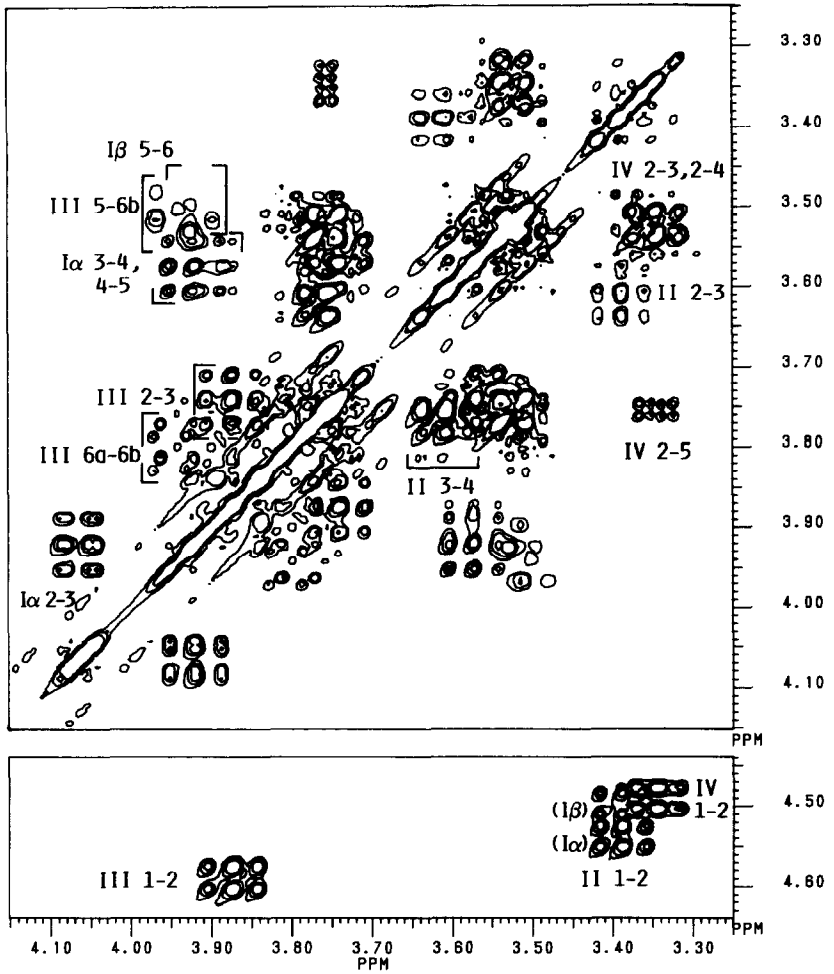


Fig. 2. 300-MHz $^1H$–$^1H$ COSY45 plot obtained at 25° for a $D_2O$ solution of the tetrasaccharide **2**. Residues are numbered as in Fig. 1., i.e., I and III (above diagonal, apart from III 1–2) denote Glc*p*NAc correlations, and II and IV denote Glc*p*A correlations (below diagonal). The Glc*p*NAc Ac and 1 H-1 signals are omitted.

form of **3**, the 4–5 cross-peaks for both Glc*p*A residues were shifted to uncrowded regions (see Fig. 3). Hence, by comparing the plots for the various compounds, the assignments indicated on Figs. 1–3 were arrived at. Most assignments were confirmed by RCT COSY experiments (plots not shown). Cross-peaks between H-2 and H-5 were observed for the terminal Glc*p*A residues of all samples studied, as indicated on Figs. 1–3 (see Discussion). However, the strong signal overlap in various regions prevented identification of all $^1H$ resonances and determination of exact shifts and coupling constants from the 300-MHz experiments alone.

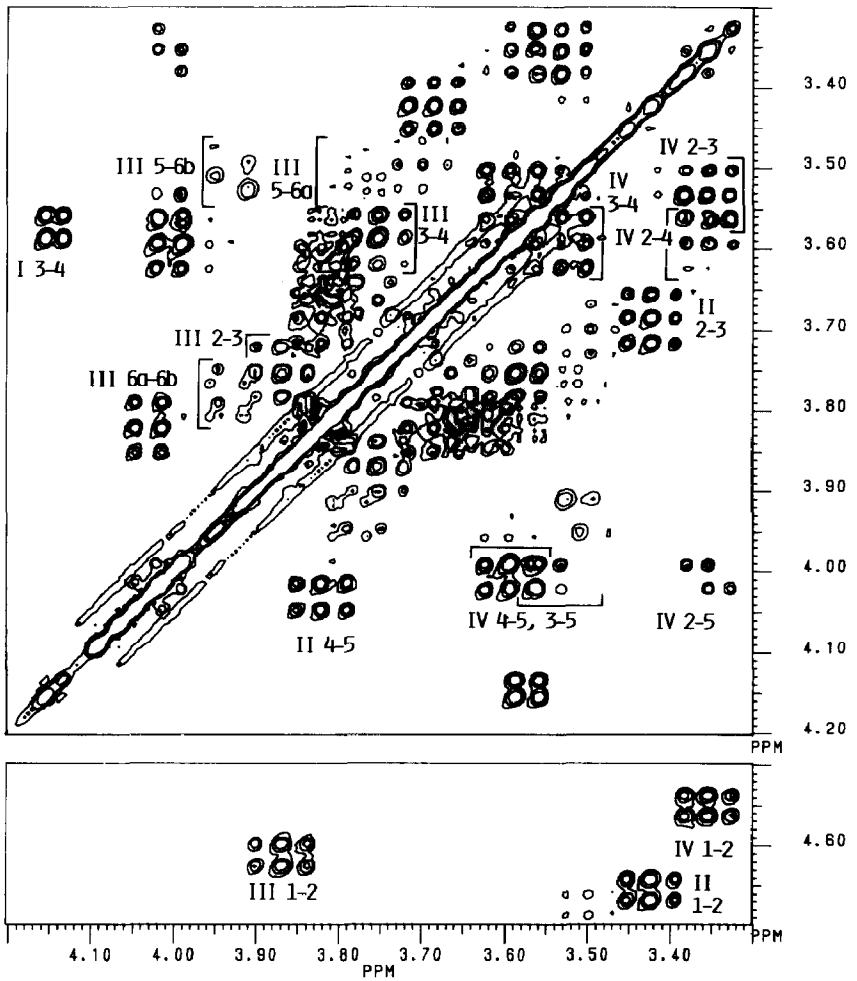


Fig. 3. 300-MHz $^1H$–$^1H$ COSY45 plot obtained at 25°C for a $D_2O$ solution of the tetrasaccharide **3** at pH 1.6. I and III (above diagonal, apart from III 1–2) denote 2-acetamido-2-deoxy-D-glucitol and Glc*p*NAc correlations, respectively; II and IV (below diagonal) denote Glc*p*A correlations. Cross-peaks for I 1a, 1b, and 2 are omitted.

Fig. 4 shows the 2D $^1H$–$^{13}C$ chemical shift contour plot obtained for **2** in $D_2O$, using inverse ($^1H$) detection. The correlations for internal residues, based on the COSY assignments for **2** (Fig. 2), have chemical shift values close to those published for hyaluronate, both for $^1H$ (ref 18) and for $^{13}C$ (ref 19). The resonances susceptible to marked end-effects were identified by comparison with the $^1H$ assignments (Figs. 1 and 2), and from a quantitative $^{13}C$ NMR spectrum acquired with inverse-gated decoupling and a long repetition time (spectrum not shown). The Glc*p*NAc I$\beta$ 1 and 2 correlations showed small shift deviations from polymer-characteristic shifts, attributed to their location at the reducing end. The Glc*p*NAc I$\alpha$ correlations for positions 1, 2, 3, and 5 deviate markedly from the

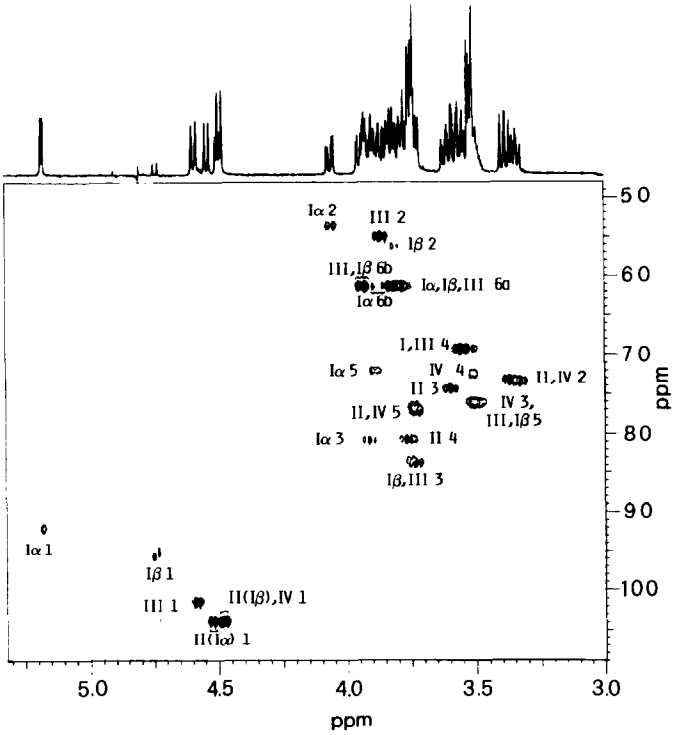


Fig. 4. A 2D $^{1}H$–$^{13}C$ chemical shift correlation spectroscopy contour plot obtained for **2** (10 mg/mL) in $D_2O$, using inverse ($^{1}H$) detection (HMQC) at 500 MHz. Symbols as for Fig. 2.

values for the polymer (which has this unit in the $\beta$ configuration). The COSY plots for **1** and **2** suggested overlap of terminal Glc*p*A H-3,4 resonances at $\delta \sim 3.5$ (see Figs. 1 and 2). This overlap is clearly seen in the heterocorrelation plot (Fig. 4). The overlap of the resonances for C-4 of Glc*p*A II and C-3 of Glc*p*NAc I$\alpha$ in the $^{13}C$ dimension ($\delta$ 80.83) could be resolved in the heteronuclear 2D plot (Fig. 4), as the corresponding $^{1}H$ frequencies differed. Thus, the data presented so far led to the assignments given in the $^{1}H$–$^{13}C$ chemical shift correlation plot (Fig. 4), and allowed exact $^{13}C$ chemical shifts to be determined from 1D spectra of **1** and **2** (Table I). The $^{13}C$ NMR shifts found for **1** confirm assignments reported in the literature[20], and the field strength used allowed the different influence of the anomeric forms of I to be detected for the C-1 and C-6 resonances of the adjacent residue II.

However, due to the overlap of some $^{1}H$ signals and to the presence of several strongly coupled spin systems, the exact $\delta$ and $J$ values could not be determined easily for **1** and **2**, neither from the 2D experiments described so far (Figs. 1, 2, and 4), nor from 1D 500-MHz spectra. From a 500-MHz COSY plot (Fig. 5), all lacking connections for **2** were identified, thus allowing the identification of all resonances in the 1D spectrum.

TABLE I

$^{13}C$ NMR data [a] ($\delta$ in ppm) for solutions of **1**, **2**, and **3** in $D_2O$

| Glc*p*NAc or derived residues | | | | | | | | | |
|---|---|---|---|---|---|---|---|---|---|
| | **1 I** [b] | | **2 I** | | **3 I** [c,d] | **3 I** [c,e] | **2 III** | **3 III** [d] | **3 III** [e] |
| | $\alpha$ | $\beta$ | $\alpha$ | $\beta$ | | | | | |
| C-1 | 91.83 | 95.51 | 91.89 | 95.58 | 63.44 | 63.57 | 101.40 | 101.87 | 101.39 |
| C-2 | 53.67 | 56.32 | 53.78 | 56.41 | 54.09 | 54.18 | 55.06 | 55.06 | 55.09 |
| C-3 | 81.29 | 83.77 | 80.83 | 83.21 | 76.46 | 76.25 | 83.86 | 83.46 | 83.85 |
| C-4 | 69.48 | 69.48 | 69.36 | 69.40 | 71.27 | 71.40 | 69.36 | 69.08 | 69.36 |
| C-5 | 72.09 | 76.29 | 72.11 | 76.30 | 71.50 | 71.40 | 76.23 | 76.16 | 76.25 |
| C-6 | 61.36 | 61.52 | 61.37 | 61.53 | 61.28 | 61.39 | 61.37 | 61.28 | 61.39 |
| C=O | 175.37 | 175.64 | 175.37 | 175.64 | 175.24 | 175.23 | 175.76 | 175.59 | 175.77 |
| $CH_3$ | 22.82 | 23.06 | 22.82 | 23.06 | 22.95 | 22.97 | 23.32 | 23.19 | 23.32 |
| Glc*p*A residues | | | | | | | | | |
| | **1 II** | | **2 II** | | **3 II** [d] | **3 II** [e] | **2 IV** | **3 IV** [d] | **3 IV** [e] |
| | (I$\alpha$) | (I$\beta$) | (I$\alpha$) | (I$\beta$) | | | | | |
| C-1 | 103.57 | 103.71 | 103.80 | 103.91 | 103.36 | 103.48 | 103.80 | 103.44 | 103.79 |
| C-2 | 73.52 | 73.52 | 73.29 | 73.29 | 73.18 | 73.54 | 73.54 | 73.27 | 73.54 |
| C-3 | 76.17 | 76.17 | 74.47 | 74.47 | 74.57 | 74.47 | 76.14 | 75.86 | 76.14 |
| C-4 | 72.52 | 72.52 | 80.83 | 80.83 | 80.78 | 80.76 | 72.53 | 71.99 | 72.53 |
| C-5 | 76.59 | 76.59 | 77.21 | 77.21 | 74.14 | 76.83 | 76.55 | 75.04 | 76.56 |
| C-6 | 176.32 | 176.36 | 175.01 | 174.97 | 172.49 | 175.12 | 176.30 | 173.11 | 176.31 |

[a] Obtained at 25°C for solutions at 10 mg/mL for **1**, and at 30 mg/mL for **2** and **3**. [b] Residues are numbered from the reducing end with Roman numerals. [c] → 3)-2-Acetamido-2-deoxy-D-glucitol. [d] Solution at pH 1.6. [e] Solution at pH 5.6.

The Glc*p*A residues at the non-reducing terminal for all the samples studied were found to yield higher-order coupling patterns as seen in the COSY plots (Figs. 1–3), due to the overlapping H-3,4 resonances. Hence, in order to obtain true chemical shift and coupling constant values, simulation and iteration of the 500-MHz 1D $^1H$ spectra was performed, as illustrated for the Glc*p*A IV spin system of **2** in Fig. 6A. The marked effect of the H-3,4 resonance overlap on the resulting subspectrum is evident, and the simulation is seen to reproduce well this detail in the experimental spectrum (Fig. 6B). The simulation of the subspectrum for Glc*p*A II confirmed that two anomeric forms of the adjacent residue gave rise to two H-3 signals at $\delta$ 3.6. Furthermore, these signals showed a further splitting in the simulated spectrum due to the strongly coupled H-4,5 shifts (Fig. 6C). This splitting, which is unresolved in the experimental spectrum, had to be taken into account in the iterative simulation to give reasonably low rms-deviation values. The chemical shifts and coupling constants obtained for **1** and **2** at convergence are given in Table II.

The remaining assignment for the $NaBH_4$-reduced tetrasaccharide, **3**, were arrived at with an approach similar to that described above for **1** and **2**, i.e., from heterocorrelation experiments and iterative simulation of 500-MHz 1D $^1H$ spectra. The resulting $^{13}C$ and $^1H$ chemical shifts are given in Tables I and II, respectively.

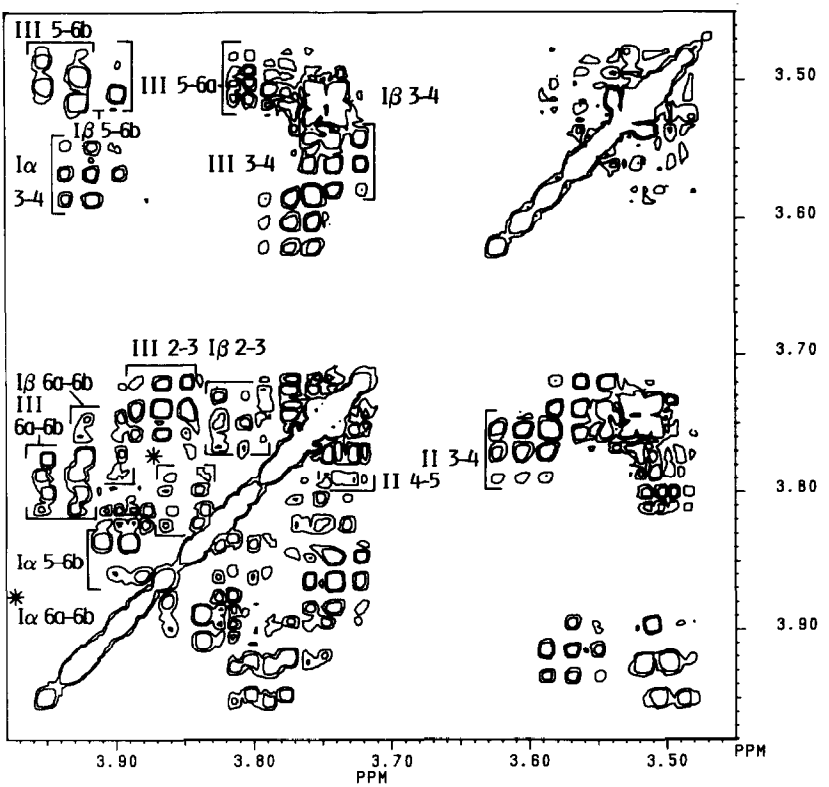


Fig. 5. Expansion of 500-MHz $^1H$–$^1H$ COSY45 contour plot for **2**. Symbols as for Fig. 2.

Fig. 7 shows $^{13}C$ NMR spectra of the tetra-, hexa-, and octa-saccharides and sodium hyaluronate in $D_2O$. Only Glc*p*NAc reducing-end signals were seen, in agreement with the known specificity of the hyaluronidase used[15].

## DISCUSSION

*Corrections to previous assignments for* **2**.—Our $^1H$ assignments for the tetrasaccharide **2** differ from those of Sugahara et al.[11] for several resonances. In general, many assignments are in disagreement with those expected from the comparison with data for the polymer[18]. This is the case for the Glc*p*NAc H-3 and H-5 resonances, which are interchanged for the $\beta$ forms (I$\beta$ and III) in their HOHAHA $^1H$ plot (their Fig. 5) and/or table (their Table 1), with respect to our results. Another discrepancy is the single shift tabulated for H-4 of the GlcA residues: we found a noticeable shift difference ($\sim$ 0.25 ppm) between the O-4 substituted (II) and the unsubstituted (IV) residues (cf. Table II). Furthermore, the Glc*p*A IV H-5 resonance has been assigned to H-4, for which we found a chemical shift almost coinciding with that of H-3 (cf. Fig. 2, Table II), as verified by the simulation (Fig. 6A).

*Deviations from first-order spectral behaviour.*—The 2–5 COSY cross-peak seen for the non-reducing terminal Glc*p*A residues caused some difficulties in the initial stages of the assignment. Normally, couplings between protons separated by 5 bonds are observed only in unsaturated systems. Hence, it is unlikely that the observed cross-peak reflects a "normal" spin–spin coupling. The H-2 resonance showed a fairly complicated, higher-order pattern in the 500-MHz 1D spectrum both for **1** and **2**. The simulated Glc*p*A IV subspectrum of **2** (Fig. 6A) demonstrated that this deceptive complexity, due to virtual coupling, originated in the strong coupling between H-3 and H-4 of this spin system. In fact, these resonances were separated sufficiently in the 500-MHz spectrum of the acid form of **3** to give a first-order dd pattern for the H-2 resonance. However, at 300 MHz, the pattern is still higher order, and the Glc*p*A IV 2–5 COSY cross-peak is present, although shifted, and the shift in H-4 also makes the presence of the 2–4 and 3–5

TABLE II

$^1$H NMR data [a] ($\delta$ in ppm, $J$ in Hz) for solutions [b] of **1**, **2**, and **3** in $D_2O$

| Residue | **1** | | | | | | **2** | | | | | |
|---|---|---|---|---|---|---|---|---|---|---|---|---|
| | | δ(Iα) | δ(Iβ) | $J$ | (Iα) | (Iβ) | | δ(Iα) | δ(Iβ) | $J$ | (Iα) | (Iβ) |
| GlcNAc I [e] | H-1 | 5.169 | 4.740 | $J_{1,2}$ | 3.55 | 8.39 | H-1 | 5.177 | 4.738 | $J_{1,2}$ | 3.49 | 8.43 |
| | H-2 | 4.051 | 3.814 | $J_{2,3}$ | 10.59 | 10.43 | H-2 | 4.058 | 3.824 | $J_{2,3}$ | 10.66 | 10.33 |
| | H-3 | 3.900 | 3.734 | $J_{3,4}$ | 8.91 | 9.58 | H-3 | 3.915 | 3.749 | $J_{3,4}$ | 8.95 | 8.58 |
| | H-4 | 3.572 | 3.539 | $J_{4,5}$ | 9.99 | 10.00 | H-4 | 3.568 | 3.532 | $J_{4,5}$ | 10.04 | 9.89 |
| | H-5 | 3.880 | 3.484 | $J_{5,6a}$ | 5.02 | 5.50 | H-5 | 3.893 | 3.496 | $J_{5,6a}$ | 5.07 | 4.90 |
| | | | | $J_{5,6b}$ | 2.44 | 2.19 | | | | $J_{5,6b}$ | 2.36 | 2.10 |
| | H-6a | 3.807 | 3.763 | $J_{6a,6b}$ | −12.39 | −12.25 | H-6a | 3.812 | 3.764 | $J_{6a,6b}$ | −12.43 | −12.48 |
| | H-6b | 3.836 | 3.901 | | | | H-6b | 3.844 | 3.909 | | | |
| | Ac | 2.028 | 2.028 | | | | Ac | 2.035 | 2.038 | | | |
| GlcA II | H-1 | 4.520 | 4.483 | $J_{1,2}$ | 7.89 | 7.89 | H-1 | 4.532 | 4.495 | $J_{1,2}$ | 7.90 | 7.90 |
| | H-2 | 3.339 | 3.339 | $J_{2,3}$ | 9.41 | 9.41 | H-2 | 3.381 | 3.381 | $J_{2,3}$ | 9.45 | 9.45 |
| | H-3 | 3.508 | 3.506 | $J_{3,4}$ | 9.05 | 9.05 | H-3 | 3.605 | 3.601 | $J_{3,4}$ | 9.00 | 9.00 |
| | H-4 | 3.509 | 3.507 | $J_{4,5}$ | 9.63 | 9.63 | H-4 | 3.768 | 3.768 | $J_{4,5}$ | 9.50 | 9.50 |
| | H-5 | 3.741 | 3.735 | | | | H-5 | 3.737 | 3.730 | | | |
| GlcNAc III | | | | | | | H-1 | | 4.584 | $J_{1,2}$ | | 8.50 |
| | | | | | | | H-2 | | 3.865 | $J_{2,3}$ | | 10.33 |
| | | | | | | | H-3 | | 3.739 | $J_{3,4}$ | | 8.75 |
| | | | | | | | H-4 | | 3.561 | $J_{4,5}$ | | 9.89 |
| | | | | | | | H-5 | | 3.498 | $J_{5,6a}$ | | 6.01 |
| | | | | | | | | | | $J_{5,6b}$ | | 2.10 |
| | | | | | | | H-6a | | 3.795 | $J_{6a,6b}$ | | −12.93 |
| | | | | | | | H-6b | | 3.937 | | | |
| | | | | | | | Ac | 2.050 | 2.048 | | | |
| GlcA IV | | | | | | | H-1 | | 4.487 | $J_{1,2}$ | | 7.89 |
| | | | | | | | H-2 | | 3.339 | $J_{2,3}$ | | 9.41 |
| | | | | | | | H-3 | | 3.516 | $J_{3,4}$ | | 9.05 |
| | | | | | | | H-4 | | 3.517 | $J_{4,5}$ | | 9.63 |
| | | | | | | | H-5 | | 3.745 | | | |

[a] Best-fit values obtained by simulation and iteration with the PANIC programme. [b] Obtained at 25°C for solutions at 10 mg/mL for **1**, and 30 mg/mL for **2** and **3**. [c] Solution at pH 1.6. [d] Solution at pH 5.6. [e] → 3)-2-Acetamido-2-deoxy-D-glucitol for **3**.

cross-peaks evident, as seen in Fig. 3. Above the simulated Glc*p*A IV subspectrum for **2** (Fig. 6A), the frequencies of the 2–5 cross-peak are indicated. Hence, it is evident that the anomalous appearance of the cross-peak with respect to that of the 1–2 cross-peak (cf. Figs. 1 and 2) is due to coherence transfer at the combination line frequencies of both resonances. Although a theoretical explanation for the observed 2–5 COSY cross-peak is lacking, it is known that in spin systems with strongly coupled subunits, coherence transfer that does not follow from the selection rules for weakly coupled spins may occur, but cannot be taken as a proof of a non-vanishing coupling[21].

*Comparison of $^{13}C$ NMR data for oligosaccharides of different length.*—The complete assignment of **1**, **2**, and **3** allowed a comparison of the $^{13}C$ chemical shifts of resonances arising from internal and terminal residues, and those of residues in an otherwise different chemical environment. In Table I, the shifts for the

| **3** [c] | | | | | | | | **3** [d] | | | | | | | |
|---|---|---|---|---|---|---|---|---|---|---|---|---|---|---|---|
| $\delta$ | | | | $J$ | | | | $\delta$ | | | | $J$ | | | |
| H-1a | 3.674 | 1b | 3.766 | $J_{1a,2}$ | 6.94 | $J_{1b,2}$ | 3.81 | H-1a | 3.656 | 1b | 3.745 | $J_{1a,2}$ | 6.80 | $J_{1b,2}$ | 4.48 |
| H-2 | 4.254 | | | $J_{1a,1b}$ | −12.17 | $J_{2,3}$ | 6.09 | H-2 | 4.250 | | | $J_{1a,1b}$ | −11.77 | $J_{2,3}$ | 6.32 |
| H-3 | 4.143 | | | $J_{3,4}$ | 1.65 | | | H-3 | 4.117 | | | $J_{3,4}$ | 1.00 | | |
| H-4 | 3.572 | | | $J_{4,5}$ | 9.39 | | | H-4 | 3.540 | | | $J_{4,5}$ | 8.77 | | |
| H-5 | 3.813 | | | $J_{5,6a}$ | 6.90 | | | H-5 | 3.825 | | | $J_{5,6a}$ | 6.50 | | |
| | | | | $J_{5,6b}$ | 3.11 | | | | | | | $J_{5,6b}$ | 2.76 | | |
| H-6a | 3.631 | | | $J_{6a,6b}$ | −12.46 | | | H-6a | 3.613 | | | $J_{6a,6b}$ | −12.20 | | |
| H-6b | 3.816 | | | | | | | H-6b | 3.822 | | | | | | |
| Ac | 2.030 | | | | | | | Ac | 2.029 | | | | | | |
| H-1 | 4.653 | | | $J_{1,2}$ | 7.88 | | | H-1 | 4.570 | | | $J_{1,2}$ | 7.85 | | |
| H-2 | 3.421 | | | $J_{2,3}$ | 9.35 | | | H-2 | 3.405 | | | $J_{2,3}$ | 9.33 | | |
| H-3 | 3.685 | | | $J_{3,4}$ | 9.20 | | | H-3 | 3.613 | | | $J_{3,4}$ | 9.32 | | |
| H-4 | 3.820 | | | $J_{4,5}$ | 9.54 | | | H-4 | 3.749 | | | $J_{4,5}$ | 9.39 | | |
| H-5 | 4.034 | | | | | | | H-5 | 3.719 | | | | | | |
| H-1 | 4.609 | | | $J_{1,2}$ | 8.56 | | | H-1 | 4.592 | | | $J_{1,2}$ | 8.52 | | |
| H-2 | 3.864 | | | $J_{2,3}$ | 10.43 | | | H-2 | 3.852 | | | $J_{2,3}$ | 9.86 | | |
| H-3 | 3.752 | | | $J_{3,4}$ | 9.86 | | | H-3 | 3.723 | | | $J_{3,4}$ | 8.62 | | |
| H-4 | 3.590 | | | $J_{4,5}$ | 10.17 | | | H-4 | 3.548 | | | $J_{4,5}$ | 9.87 | | |
| H-5 | 3.497 | | | $J_{5,6a}$ | 5.70 | | | H-5 | 3.469 | | | $J_{5,6a}$ | 5.25 | | |
| | | | | $J_{5,6b}$ | 2.70 | | | | | | | $J_{5,6b}$ | 1.89 | | |
| H-6a | 3.777 | | | $J_{6a,6b}$ | −12.35 | | | H-6a | 3.782 | | | $J_{6a,6b}$ | −12.73 | | |
| H-6b | 3.924 | | | | | | | H-6b | 3.922 | | | | | | |
| Ac | 2.003 | | | | | | | Ac | 2.029 | | | | | | |
| H-1 | 4.548 | | | $J_{1,2}$ | 7.88 | | | H-1 | 4.470 | | | $J_{1,2}$ | 7.90 | | |
| H-2 | 3.353 | | | $J_{2,3}$ | 9.43 | | | H-2 | 3.324 | | | $J_{2,3}$ | 9.40 | | |
| H-3 | 3.533 | | | $J_{3,4}$ | 9.13 | | | H-3 | 3.499 | | | $J_{3,4}$ | 9.00 | | |
| H-4 | 3.583 | | | $J_{4,5}$ | 9.96 | | | H-4 | 3.500 | | | $J_{4,5}$ | 9.49 | | |
| H-5 | 4.007 | | | | | | | H-5 | 3.729 | | | | | | |

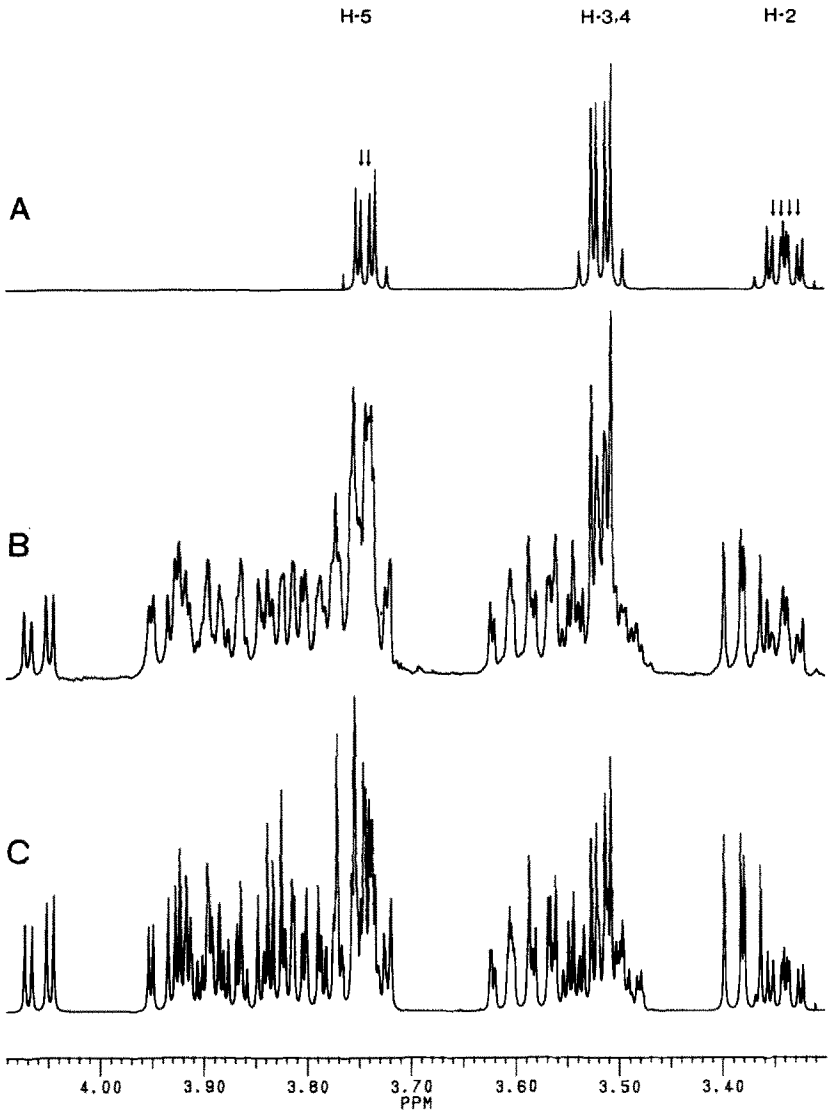


Fig. 6. Experimental and simulated 500-MHz $^1$H NMR spectra obtained for **2** in $D_2O$: A, simulated Glc*p*A IV subspectrum, the frequencies of the 2–5 COSY cross-peak are indicated; B, experimental spectrum; C, simulated spectrum for **2** assuming $\alpha/\beta$ ratio 3:2. Simulations were performed with the PANIC software (Bruker), H-1 and Ac signals are omitted from the plots.

resonances of the non-reducing Glc*p*A residues **1** II, **2** IV, and **3** IV (pH 5.6) are seen to yield nearly identical shifts for all carbons, regardless of the oligosaccharide length and composition. Only the C-1 resonances of the Glc*p*A residues are slightly influenced by the nature of the adjacent Glc*p*NAc residue (cf. Fig. 7). Likewise, the internal Glc*p*NAc residues III of **2** and **3** gave identical shifts for all resonances, whereas the reducing-end residues (I) of **1** and **2** gave pairwise similar

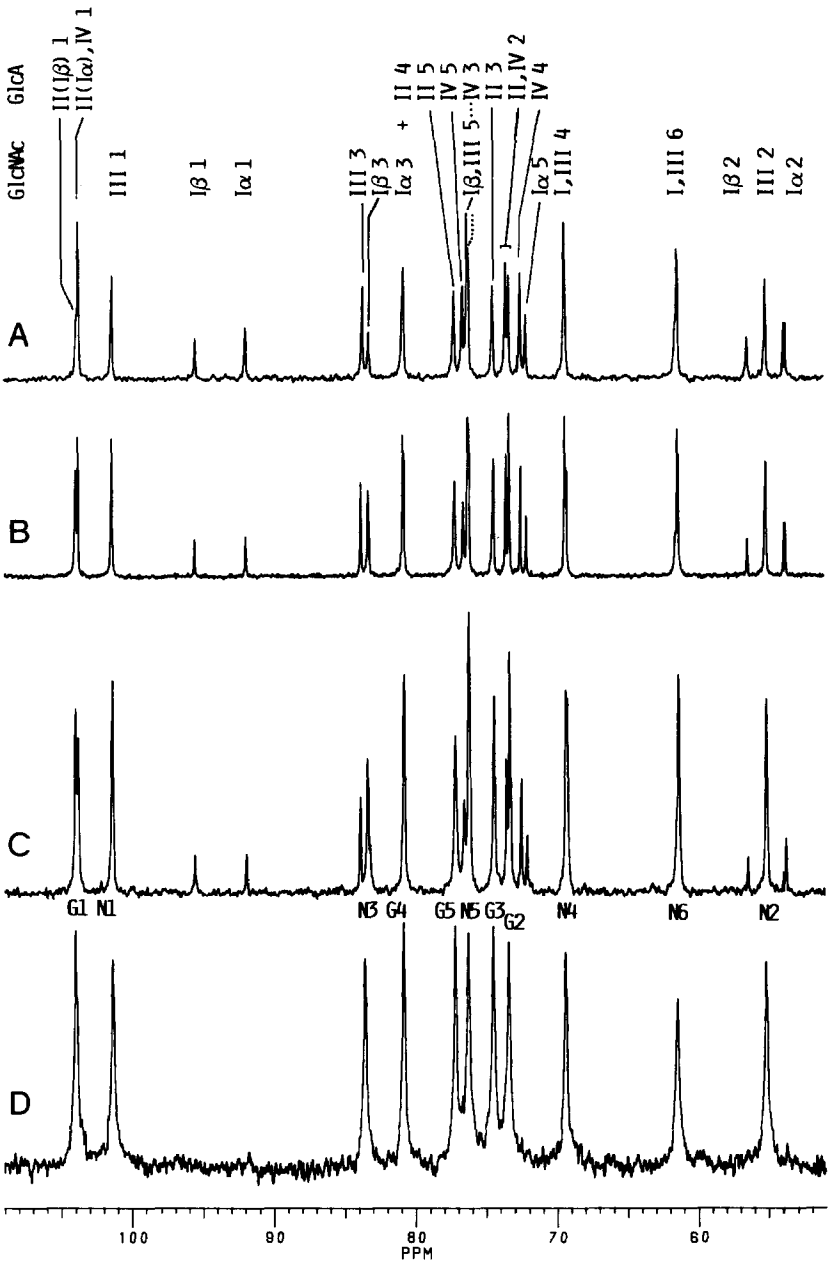


Fig. 7. 50.3-MHz $^{13}C$ NMR spectra of $D_2O$ solutions of hyaluronate and derived oligosaccharides obtained by testicular hyaluronidase digestion: A, tetrasaccharide; B, hexasaccharide; C, octasaccharide. Assignments are indicated for the tetrasaccharide **2** (A) and for the hyaluronate polymer (D), for which N and G denote Glc*p*NAc and Glc*p*A residues, respectively. Acetyl and carboxyl resonances are omitted from plots.

shifts for all $\alpha$- and $\beta$-form resonances, except for C-3, which gave a $\sim 0.5$ ppm lower shift for **2** than for **1**. This difference reflects the fact that Glc*p*NAc C-3, which is involved in the glycosidic bond to the adjacent Glc*p*A residue, is sensitive to the different nature of these residues, which is terminal for **1** and internal for **2**. Indeed, the $\delta$ value for **1** I$\beta$ C-3 is seen to agree better with that of the III C-3 of **2**, both residues being adjacent to non-reducing terminal Glc*p*A residues. The C-3 resonance of the Glc*p*NAc I$\beta$ spin systems of **2**, together with those of the residues III of the hexasaccharide and III and V of the octasaccharide, are seen to give chemical shifts almost coinciding with those of the polymer (Fig. 7). Hence, the shift deviations seen for the shorter oligosaccharides can be explained by the presence of the terminal residues. Likewise, induced shifts were seen on their adjacent internal residues at both ends, with respect to the polymer-characteristic shifts. This explains why the internal disaccharide units for the hexa- and octa-saccharide were seen to give polymer-like chemical shifts for all resonances, with intensities which increase systematically throughout the series. Hence, to the extent that $^{13}C$ shifts reflects conformational features, our observations suggest that the average segmental conformation for the polymer in water equals that of comparable sections of the oligosaccharides.

*Hydrogen bonding and conformational stabilisation.*—Various intramolecular hydrogen bonds have been postulated for hyaluronate, based on NMR studies[8,9,18] and periodate oxidation rates[22], although the reaction order and the interpretation of the periodate oxidation data have been questioned[23]. In particular, a cooperative set of hydrogen bonds involving the acetamido NH and C=O functions of a Glc*p*NAc residue, and the $COO^-$ and the HO-2 groups, respectively, of the Glc*p*A residues on each side has been suggested[7,8], also postulating the presence of a water-bridged hydrogen bond between the NH and carboxylate groups[9]. It has been suggested that hydrogen bonds stabilise the hyaluronate conformation, and contribute to its stiffness[22].

Several relevant observations were made in the present work. Firstly, the shifts for the resonances of the non-reducing Glc*p*A residues show nearly identical shifts for all carbons, regardless of the oligosaccharide length and composition. Hence, if a hydrogen bond is formed between the HO-2 of the Glc*p*A residue and the C=O of the acetamido group, its formation is not likely to depend on the presence of a further bond involving the NH and the carboxylate of the adjacent Glc*p*A residue. Secondly, the chemical shift values reported[20] for the Glc*p*NAc residue of a modified trisaccharide derived from hyaluronate, $\beta$-D-Glc*p*A-(1 → 3)-$\beta$-D-Glc*p*NAc-(1 → 3)-D-arabinaric acid (in the sodium salt form), were all in agreement with those of the internal Glc*p*NAc III residues of **2** and **3**. For the latter, the suggested hydrogen bond pattern could form in principle, whereas it is unlikely that the former gains any stabilising effect from hydrogen bonding to the arabinarate residue. Furthermore, other NMR data have suggested that hydrogen bonds involving the acetamido group are more important for the hyaluronate conformation in methyl sulfoxide[8,12] than in water[9,10]. In $H_2O$, the NH $^1H$ resonances of

both internal and terminal Glc*p*NAc residues gave coupling constants suggesting similar orientations of their acetamido groups[10].

Hence, our observations do not suggest any significant role for cooperative hydrogen bonding involving the acetamido group in the determination of the hyaluronate conformation in water. Similar conclusions, i.e., that the hyaluronate conformation does not seem to be stabilised to any appreciable extent by cooperative interactions involving several residues, were drawn from CD studies[24].

## NOTE ADDED IN PROOF

While this article was in press, a Note reporting NMR data for the tetrasaccharide 2 has appeared (P. Livant, L. Rodén, and N.R. Krishna, *Carbohydr. Res.*, 237 (1992) 271–281). However, the pH applied was lower than in the present study and the different experimental conditions explain the differences seen in the reported chemical shifts. Nevertheless, taking into account these differences, some of the $^{13}C$ assignments are at variance with our findings. We did not observe an anomeric twinning effect on the C-1 of GlcNAc III, and we believe that their shift value assigned to C-1 of GlcNAc III(I$\beta$) is wrong, and that this resonance is found at the shift given for III(I$\alpha$) in their Table II. Furthermore, the GlcNAc I$\alpha$ C-5 resonance is found near the GlcA IV C-4 resonance, which consists of only one signal (cf. the HMQC plot in our Fig. 4). Their suggestion that the splitting pattern seen for Glc*p*A IV H-2 is due to a mixture of conformers (e.g., chair and twist-boat), can be excluded from the simulated subspectrum, which convincingly demonstrates the presence of virtual coupling (i.e., higher order) deriving from the overlap of the chemical shifts H-3 and H-4 of this spin system (see our Fig. 6 and Discussion). Likewise, the higher order of this spin system implies that one cannot take the H-2/H-5 COSY cross-peak observed for this spin system as a proof for the presence of a 5-bond coupling (see Discussion).

## ACKNOWLEDGMENTS

We thank the Istituto di Radiologia, Università degli Studi di Trieste, and the Dipartimento di Scienze e Tecnologie Biomediche, Università di Udine, for access to the Bruker AM 300 WB and AM 500 instruments, respectively. We are grateful to Dr. P. Dvortsak, Bruker Anlytische Messtechnik GmbH, Rheinstetten, for performing the 2D $^{1}H-^{13}C$ HMQC experiments, and to T. Skjetne, at the MR Centre, Trondheim, for useful discussions. A fellowship from the Area di Ricerca, Trieste (to RT) is gratefully acknowledged.

## REFERENCES

1 T.E. Hardingham and H.M. Muir, *Biochim. Biophys. Acta*, 279 (1972) 401–405.
2 T.C. Laurent, in E.A. Balazs (Ed.), *Chemistry and Molecular Biology of the Extracellular Matrix*, Academic, New York, 1970, pp 703–732.

3 E.A. Balazs, in A. Helfet (Ed.), *Disorders of the Knee*, Lippincott, Philadelphia, 1974, pp 63–75.
4 H. Sato, T. Takahashi, I. Hirotsugu, T. Fukushima, M. Tabata, F. Sekine, K. Kobayashi, M. Negishi, and Y. Niwa, *Arthritis Rheumat.*, 31 (1988) 63–71.
5 D.C. West, I.N. Hampson, F. Arnold, and S. Kumar, *Science*, 228 (1985) 1324–1326.
6 J.E. Scott and F. Heatley, *Biochem. J.*, 181 (1979) 445–449.
7 J.E. Scott, F. Heatley, D. Moorcroft, and A.H. Olavesen, *Biochem. J.*, 199 (1981) 829–832.
8 J.E. Scott, F. Heatley, and W. Hull, *Biochem. J.*, 220 (1984) 197–205.
9 F. Heatley and J.E. Scott, *Biochem. J.*, 254 (1988) 489–493.
10 M.K. Cowman, D. Cozart, N. Nakanishi, and E.A. Balazs, *Arch. Biochem. Biophys.*, 230 (1984) 203–212.
11 K. Sugahara, S. Yamada, M. Sugiura, K. Takeda, R. Yuen, H.E. Khoo, and C.H. Poh, *Biochem. J.*, 283 (1992) 99–104.
12 B.J. Kvam, M. Atzori, R. Toffanin, S. Paoletti, and F. Biviano, *Carbohydr. Res.*, 230 (1992) 1–13.
13 A. Bax and S. Subramanian, *J. Magn. Reson.*, 67 (1986) 565–569.
14 S. Castellano and A.A. Bothner-By, *J. Chem. Phys.*, 41 (1964) 3863–3869.
15 B. Weissmann, K. Meyer, P. Sampson, and A. Linker, *J. Biol. Chem.*, 208 (1954) 417–429.
16 N. Blumenkrantz and G. Asboe-Hansen, *Anal. Biochem.*, 54 (1973) 484–489.
17 T. Bitter and H.M. Muir, *Anal. Biochem.*, 4 (1962) 330–333.
18 D. Welti, D.A. Rees, and E.J. Welsh, *Eur. J. Biochem.*, 94 (1979) 505–514.
19 S.M. Bociek, A.H. Darke, D. Welti, and D.A. Rees, *Eur. J. Biochem.*, 109 (1980) 447–456.
20 Y. Inoue and K. Nagasawa, *Carbohydr. Res.*, 141 (1985) 99–110.
21 R. Ernst, G. Bodenhausen, and A. Wokaun, *Principles of Nuclear Magnetic Resonance in One and Two Dimensions*, Clarendon, Oxford, 1987, p 426.
22 J.E. Scott and M.J. Tigwell, *Biochem. J.*, 173 (1978) 103–114.
23 N. Ueno and B. Chakrabarti, *Biopolymers*, 28 (1989) 1891–1902.
24 M.K. Cowman, E.A. Balazs, C.W. Bergman, and K. Meyer, *Biochemistry*, 20 (1981) 1379–1385.